



Chemokine (C-C Motif) Ligand 1 Derived from Tumor-Associated Macrophages Contributes to Esophageal Squamous Cell Carcinoma Progression via CCR8-Mediated Akt/Proline-Rich Akt...

Fujikawa, Masataka ; Koma, Yu-ichiro ; Hosono, Masayoshi ; Urakawa, Naoki ; Tanigawa, Kohei ; Shimizu, Masaki ; Kodama, Takayuki ;...

(Citation)

American Journal of Pathology, 191(4):686-703

(Issue Date)

2021-04

(Resource Type)

journal article

(Version)

Version of Record

(Rights)

© 2021 American Society for Investigative Pathology. Published by Elsevier Inc.
This is an open access article under the CC BY-NC-ND license
(<http://creativecommons.org/licenses/by-nc-nd/4.0>).

(URL)

<https://hdl.handle.net/20.500.14094/90008149>





IMMUNOPATHOLOGY AND INFECTIOUS DISEASES

Chemokine (C-C Motif) Ligand 1 Derived from Tumor-Associated Macrophages Contributes to Esophageal Squamous Cell Carcinoma Progression via CCR8-Mediated Akt/Proline-Rich Akt Substrate of 40 kDa/Mammalian Target of Rapamycin Pathway



Masataka Fujikawa,^{*†} Yu-ichiro Koma,^{*} Masayoshi Hosono,[†] Naoki Urakawa,[†] Kohei Tanigawa,^{*†} Masaki Shimizu,^{*†} Takayuki Kodama,^{*} Hiroki Sakamoto,^{*†} Mari Nishio,^{*} Manabu Shigeoka,^{*} Yoshihiro Kakeji,[†] and Hiroshi Yokozaki^{*}

From the Division of Pathology,^{*} Department of Pathology, and the Division of Gastro-intestinal Surgery,[†] Department of Surgery, Kobe University Graduate School of Medicine, Kobe, Japan

Accepted for publication
January 6, 2021.

Address correspondence to
Yu-ichiro Koma, M.D., Ph.D.,
Division of Pathology, Department of Pathology, Kobe University Graduate School of Medicine, 7-5-1 Kusunoki-cho, Chuo-ku, Kobe 650-0017, Japan. E-mail: koma@med.kobe-u.ac.jp.

Tumor-associated macrophages (TAMs) promote tumor progression. The number of infiltrating TAMs is associated with poor prognosis in esophageal squamous cell carcinoma (ESCC) patients; however, the mechanism underlying this phenomenon is unclear. cDNA microarray analysis indicates that the expression of chemokine (C-C motif) ligand 1 (*CCL1*) is up-regulated in peripheral blood monocyte-derived macrophages stimulated using conditioned media from ESCC cells (TAM-like macrophages). Here, we evaluated the role of *CCL1* in ESCC progression. *CCL1* was overexpressed in TAM-like macrophages, and *CCR8*, a *CCL1* receptor, was expressed on ESCC cell surface. TAM-like macrophages significantly enhanced the motility of ESCC cells, and neutralizing antibodies against *CCL1* or *CCR8* suppressed this increased motility. Recombinant human *CCL1* promoted ESCC cell motility via the Akt/proline-rich Akt substrate of 40 kDa/mammalian target of rapamycin pathway. Phosphatidylinositol 3-kinase or Akt inhibitors, *CCR8* silencing, and neutralizing antibody against *CCR8* could significantly suppress these effects. The overexpression of *CCL1* in stromal cells or *CCR8* in ESCC cells was significantly associated with poor overall survival ($P = 0.002$ or $P = 0.009$, respectively) and disease-free survival ($P = 0.009$ or $P = 0.047$, respectively) in patients with ESCC. These results indicate that the interaction between stromal *CCL1* and *CCR8* on cancer cells promotes ESCC progression via the Akt/proline-rich Akt substrate of 40 kDa/mammalian target of rapamycin pathway, thereby providing novel therapeutic targets. (*Am J Pathol* 2021, 191: 686–703; <https://doi.org/10.1016/j.ajpath.2021.01.004>)

Esophageal cancer is the seventh most common cancer and the sixth leading cause of cancer-related deaths, accounting for an estimated 572,000 new cases worldwide and approximately 509,000 deaths in 2018.¹ Esophageal squamous cell carcinoma (ESCC) is the most common histologic subtype of esophageal cancer in Eastern Asia and Southern and Eastern Africa.^{1,2} Alcoholic beverages, smoking, and hot foods are the risk factors for ESCC.^{3,4} ESCC is recognized as a highly refractory cancer. It may be caused by anatomic and histologic characteristics of the esophagus.^{5,6} The esophagus runs along the dorsal neck and

mediastinum without a serosal barrier. In the mediastinum, the esophagus is adjacent to important organs, including the trachea, aortic arch, right pulmonary artery, pericardium, left atrium, vertebral column, and pleura. In addition, many venous and lymphatic vessels transverse the esophageal submucosa.⁶ Therefore, ESCC is associated with high rates

Supported by Japan Society for the Promotion of Science grants-in-aid for scientific research 17K08693 (H.Y.), 18K07015 (Y.-i.K.), and 20K07373 (H.Y.).

Disclosures: None declared.

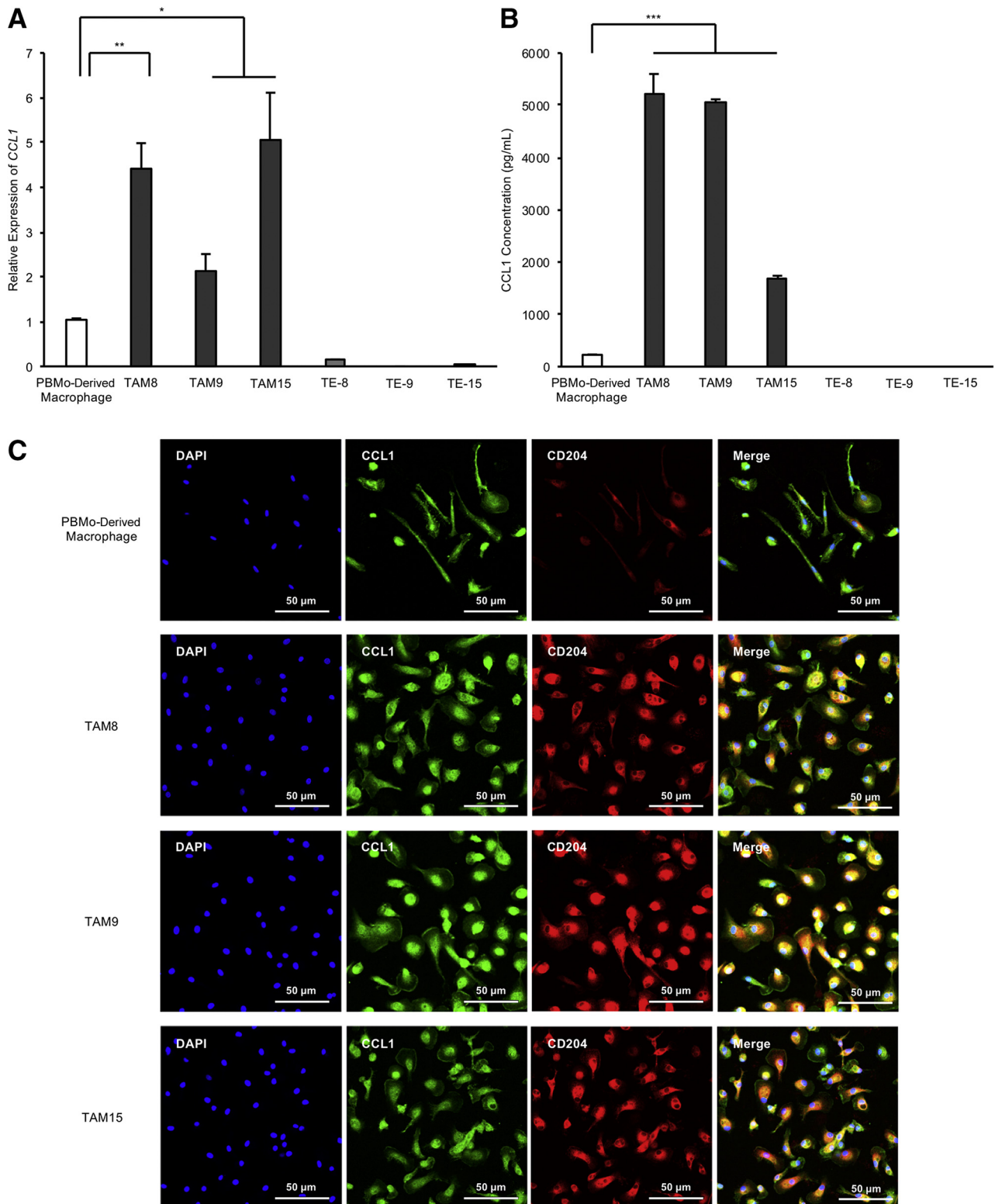
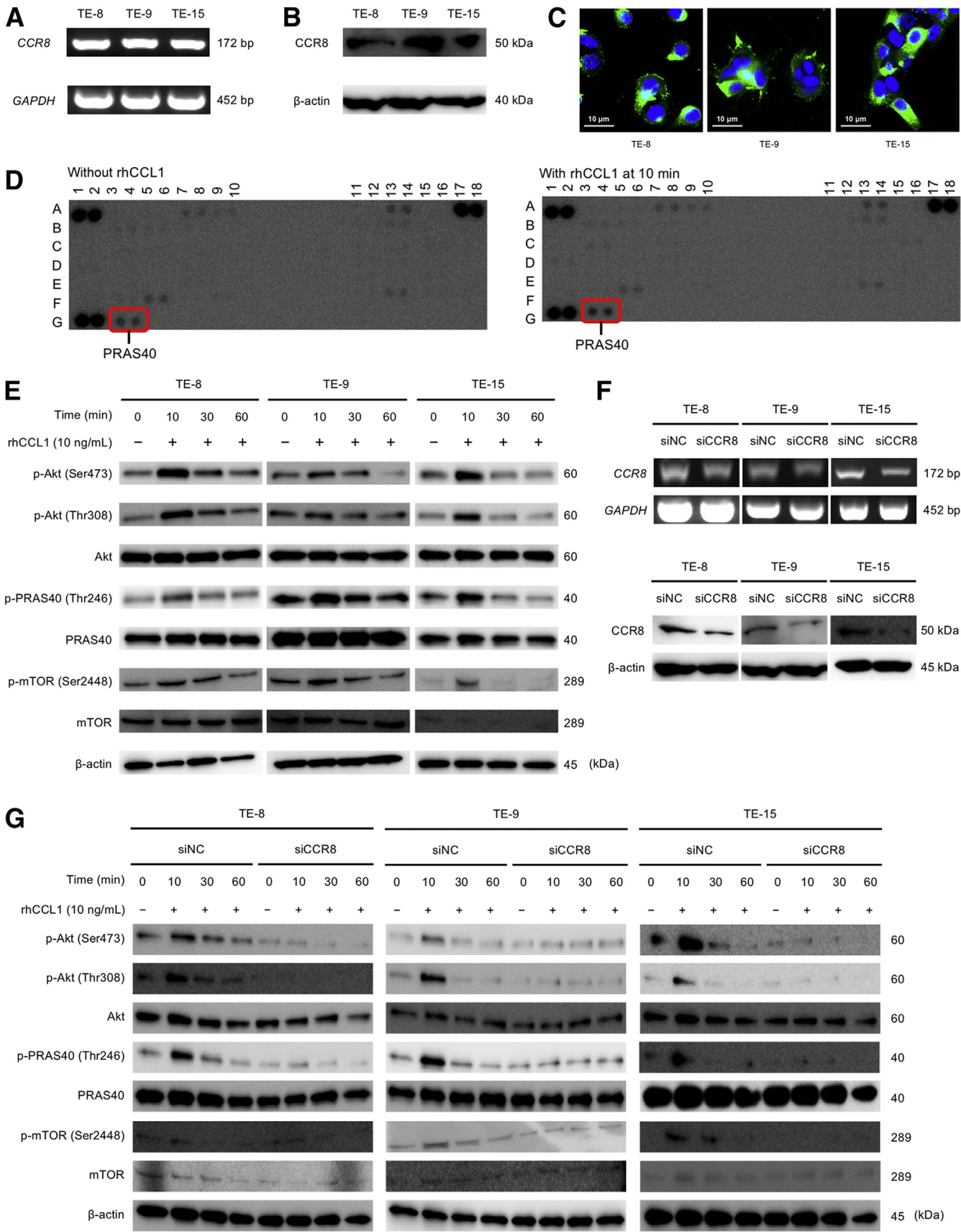


Figure 1 Up-regulation of chemokine (C-C motif) ligand 1 (CCL1) expression in tumor-associated macrophage (TAM)-like macrophages. **A:** Expression of *CCL1* mRNA in peripheral blood monocyte (PBMo)-derived macrophages, TAM-like macrophages (TAM8, TAM9, and TAM15), and TE-8, TE-9, and TE-15 cells was determined using quantitative real-time PCR. Data were normalized to *GAPDH* levels (internal control). Assays were performed in triplicate. **B:** CCL1 concentration in the supernatant of PBMo-derived macrophages, TAM-like macrophages (TAM8, TAM9, and TAM15), and TE-8, TE-9, and TE-15 cells. Protein levels were measured using an enzyme-linked immunosorbent assay. Assays were performed in triplicate. **C:** Expression of CCL1 in PBMo-derived macrophages and TAM-like macrophages (TAM8, TAM9, and TAM15) was confirmed by immunofluorescence using an anti-CCL1 antibody (green). Nuclei were stained with DAPI (blue). Macrophages were stained using an anti-CD204 antibody (red). Data are expressed as means \pm SEM (**A** and **B**). * $P < 0.05$, ** $P < 0.01$, and *** $P < 0.001$. Scale bars = 50 μ m (**C**).



of infiltration and metastasis. Despite improvements in treatments for ESCC, including surgery, chemotherapy, and radiotherapy, patient prognosis is still poor, with a 5-year overall survival (OS) rate of 10% to 20%.^{7,8} To improve the patient outcomes, further investigations aimed at clarifying the mechanisms underlying tumor progression are warranted.

The tumor microenvironment consists of cancer cells and stromal cells such as macrophages, fibroblasts, lymphocytes, and vascular endothelial cells. It contributes to tumor progression in several cancers, including that in ESCC.^{9,10} Interactions between cancer cells and stromal cells in the tumor microenvironment play an important role in promoting tumor progression.¹¹ Macrophages, that are abundantly present in the tumor microenvironment, have two different phenotypes—tumor-suppressive and tumor-progressive. Tumor-associated macrophages (TAMs) differentiate into the tumor-progressive type and accelerate tumor malignancy.^{12–14} TAMs express specific molecules, such as CD163 and CD204, which are used as tumor-progressive macrophage markers.^{15,16} CD204-positive TAMs are associated with poor prognosis in lung cancer,¹⁷ ovarian cancer,¹⁸ bladder cancer,¹⁹ and breast cancer.²⁰ Increase in the number of CD204-positive TAMs at the tumor site is significantly correlated with a poor prognosis in patients with ESCC.²¹ However, the role of TAMs in ESCC remains unclear. To further investigate the interaction between TAMs and ESCC cells, we had previously employed cDNA microarray analysis to compare gene expression between peripheral blood monocyte (PBMo)—derived macrophages and PBMo-derived macrophages stimulated using conditioned media (CM) from ESCC cells (TAM-like macrophages).²² Several proteins whose expression was up-regulated in TAM-like macrophages, such as growth factor,^{22,23} adhesion molecule,²⁴ and chemokines,^{25,26} may be related to tumor progression in ESCC.

The present study focused on chemokine (C-C motif) ligand 1 (*CCL1*), which is up-regulated in TAM-like macrophages compared with that in PBMo-derived macrophages. *CCL1* is a chemokine that attracts monocytes,

helper T cells, and regulatory T cells (Tregs)^{27,28} and selectively interacts with CCR8.²⁹ CCR8 is a member of the β chemokine receptor family and is a seven-transmembrane protein, similar to G-protein–coupled receptors.³⁰ Type 2 helper T cells, Tregs, and monocytes express CCR8.³¹ The CCL1-CCR8 axis promotes the recruitment and activation of T cells in inflammatory conditions, such as dextran sulfate sodium–induced colitis,³² asthma,³³ and atopic dermatitis.³⁴ The CCL1-CCR8 axis also contributes to tumor progression in breast cancer, melanoma, bladder cancer, and renal cancer.^{35,36} However, the role of the CCL1-CCR8 axis in ESCC progression has not been established. The aim of this study was to determine the role of TAM-derived CCL1 in the ESCC microenvironment.

Materials and Methods

Cell Lines and Cell Cultures

Three ESCC cell lines (TE-8, TE-9, and TE-15) were obtained from the RIKEN BioResource Center (Tsukuba, Japan). TE-8 cells are moderately differentiated ESCC cells; TE-9 cells are poorly differentiated ESCC cells; and TE-15 cells are well-differentiated ESCC cells.³⁷ ESCC cell lines with different degrees of differentiation were selected to demonstrate that all of the *in vitro* results were applicable to various types of ESCC. Cells were authenticated using short tandem repeat analysis at RIKEN and at the Cell Resource Center for Biomedical Research, Institute of Development, Aging and Cancer, Tohoku University (Sendai, Japan) in 2009 and 2010. TE-8, TE-9, and TE-15 cells were confirmed to be mycoplasma-negative using a Venor Gem Classic Mycoplasma Detection Kit (Minerva Biolabs, Berlin, Germany). TE-8, TE-9, and TE-15 cells were maintained in RPMI 1640 (Wako, Osaka, Japan) medium supplemented with 10% fetal bovine serum (FBS; Sigma-Aldrich, St. Louis, MO) and 1% antibiotic-antimycotic (Invitrogen, Carlsbad, CA). CM of TE-8, TE-9, and TE-15 cells was prepared by seeding 5×10^6 tumor cells per 10 mL of complete medium in 100-mm dishes for 24

Figure 2 The Akt/proline-rich Akt substrate of 40 kDa (PRAS40)/mammalian target of rapamycin (mTOR) signaling pathway was activated in TE-8, TE-9, and TE-15 cells in response to the binding of chemokine (C-C motif) ligand 1 (*CCL1*) to CCR8. **A:** The expression of *CCR8* mRNA in TE-8, TE-9, and TE-15 cells was confirmed using RT-PCR. *GAPDH* was used as an internal control. **B:** CCR8 expression in TE-8, TE-9, and TE-15 cells was confirmed by Western blot analysis. β -Actin was used as an internal control. **C:** The expression of CCR8 in TE-8, TE-9, and TE-15 cells was confirmed by immunofluorescence using an anti-CCR8 antibody (green). Nuclei were stained with DAPI (blue). **D:** Comparison of the levels of various phosphorylated proteins between TE-8 cells treated with and without recombinant human CCL1 (rhCCL1; 10 ng/mL) for 10 minutes. **E:** Changes in the levels of phosphorylated and total Akt, PRAS40, and mTOR in TE-8, TE-9, and TE-15 cells after rhCCL1 treatment (10 ng/mL). TE-8, TE-9, and TE-15 cells in serum-free conditions were treated with rhCCL1 (10 ng/mL) for 0, 10, 30, and 60 minutes. Western blot analysis for Akt, phosphorylated Akt (p-Akt; Ser473), p-Akt (Thr308), PRAS40, phosphorylated PRAS40 (p-PRAS40; Ser248), mTOR, phosphorylated mTOR (p-mTOR; Ser2448), and β -actin was performed using total protein extracted from these cells. **F:** Confirmation of the effect of CCR8 knockdown on TE-8, TE-9, and TE-15 cells using siRNAs against CCR8 (siCCR8; 20 nmol/L). Cells transfected with negative control siRNAs (siNCs) were used as the negative control. Effective knockdown of CCR8 was confirmed by RT-PCR (internal control: *GAPDH*) and Western blot analysis (internal control: β -actin). **G:** Changes in the levels of phosphorylated and total Akt, PRAS40, and mTOR in TE-8, TE-9, and TE-15 cells transfected with siNC or siCCR8 after rhCCL1 treatment (10 ng/mL). siNC- or siCCR8-transfected TE-8, TE-9, and TE-15 cells in serum-free conditions were treated with rhCCL1 (10 ng/mL) for 0, 10, 30, and 60 minutes. Western blot analysis for Akt, p-Akt (Ser473), p-Akt (Thr308), PRAS40, p-PRAS40 (Ser248), mTOR, p-mTOR (Ser2448), and β -actin was performed using total protein extracted from these cells. Cells transfected with siNCs were used as the negative control. Scale bars = 10 μ m (**C**).

Table 1 The Coordinates of Capture Antibodies in the Proteome Profiler Human Phospho-Kinase Array Kit

Coordinate	Target	Coordinate	Target
A-1, A-2	Reference spot	D-9, D-10	STAT5a
A-3, A-4	p38 α	D-11, D-12	p70 S6 kinase
A-5, A-6	ERK1/2	D-13, D-14	RSK 1/2/3
A-7, A-8	JNK 1/2/3	D-15, D-16	eNOS
A-9, A-10	GSK-3 α / β	E-1, E-2	Fyn
A-13, A-14	p53	E-3, E-4	Yes
A-17, A-18	Reference spot	E-5, E-6	Fgr
B-3, B-4	EGF R	E-7, E-8	STAT6
B-5, B-6	MSK1/2	E-9, E-10	STAT5b
B-7, B-8	AMPK α 1	E-11, E-12	STAT3
B-9, B-10	Akt 1/2/3	E-13, E-14	p27
B-11, B-12	Akt 1/2/3	E-15, E-16	PLC- γ 1
B-13, B-14	p53	F-1, F-2	Hck
C-1, C-2	TOR	F-3, F-4	Chk-2
C-3, C-4	CREB	F-5, F-6	FAK
C-5, C-6	HSP27	F-7, F-8	PDGF R β
C-7, C-8	AMPK α 2	F-9, F-10	STAT5a/b
C-9, C-10	β -Catenin	F-11, F-12	STAT3
C-11, C-12	p70 S6 kinase	F-13, F-14	WNK1
C-13, C-14	p53	F-15, F-16	PYK2
C-15, C-16	c-Jun	G-1, G-2	Reference spot
D-1, D-2	Src	G-3, G-4	PRAS40
D-3, D-4	Lyn	G-9, G-10	PBS
D-5, D-6	Lck	G-11, G-12	HSP60
D-7, D-8	STAT2	G-17, G-18	PBS

AMPK α 1, 5' AMP-activated protein kinase α -1; AMPK α 2, 5' AMP-activated protein kinase α -2; CREB, cyclic AMP-responsive element binding protein; EGF R, epidermal growth factor receptor; eNOS, endothelial nitric oxide synthase; ERK1/2, extracellular signal-regulated kinase 1/2; FAK, focal adhesion kinase; GSK-3 α / β , glycogen synthase kinase-3 α / β ; HSP, heat shock protein; JNK, c-Jun N-terminal kinase; Lck, lymphocyte-specific protein tyrosine kinase; MSK1/2, mitogen- and stress-activated kinases 1/2; PBS, phosphate-buffered saline; PDGF R β , platelet-derived growth factor receptor β ; PLC, phospholipase C; PRAS40, proline-rich Akt substrate of 40 kDa; PYK2, proline-rich tyrosine kinase 2; RSK 1/2/3, ribosomal protein S6 kinase 1/2/3; TOR, target of rapamycin; WNK1, with-no-lysine kinase 1.

hours, and the medium was replaced with complete Dulbecco's modified Eagle's medium (Wako) supplemented with 10% human AB serum (Lonza, Walkersville, MD). After incubation for 48 hours, the supernatants were harvested, centrifuged, and stored in aliquots at -80°C .

Macrophage Cultures

Peripheral blood mononuclear cells were collected from healthy volunteer donors after obtaining informed consent. The autoMACS Pro Separator (Miltenyi Biotec, Bergish Gladbach, Germany) was used to separate CD14⁺ PBMs from peripheral blood mononuclear cells based on positive selection. PBMs were incubated with macrophage colony-stimulating factor (R&D Systems, Minneapolis, MN; 25 ng/mL) for six days to induce the formation of PBMo-derived macrophages and cultured for two days with 50% CM of

TE-8, TE-9, and TE-15 cells to achieve TAM-like polarization, as demonstrated in our previous studies.²¹ PBMo-derived macrophages stimulated with CM of TE-8, TE-9, or TE-15 cells were defined as TAM-like PBMo-derived macrophages (TAM8, TAM9, or TAM15, respectively).

Tissue Samples

A total of 69 human ESCC tissue samples, which were surgically removed at Kobe University Hospital (Kobe, Japan) from 2005 to 2010, were used in this study. None of the patients had received adjuvant chemotherapy or radiotherapy before surgery. Informed consent for the use of tissue samples was obtained from all patients, and the study was approved by the Institutional Review Board of Kobe University. All specimens were fixed with 10% formalin and embedded in paraffin wax. Histologic and clinicopathologic parameters were analyzed using the Japanese Classification of Esophageal Cancer, proposed by the Japan Esophageal Society,³⁸ and the TNM classification, proposed by the Union for International Cancer Control.³⁹

RT-PCR and Quantitative Real-Time PCR

Total RNA was extracted from cultured cells using the RNeasy Mini Kit (Qiagen, Hilden, Germany). The expression of *CCR8* and the internal control gene, glyceraldehyde-3-phosphate dehydrogenase (*GAPDH*), was evaluated using RT-PCR. The PCR products were subjected to electrophoresis on a 2% agarose gel. Quantitative real-time PCR for *CCL1* and *GAPDH* was performed using the ABI StepOne Real-Time PCR System (Applied Biosystems, Foster City, CA). The C_T values were determined by plotting the observed fluorescence against the cycle number. C_T values were analyzed using the comparative C_T method and normalized to those of *GAPDH*.

Relative gene expression was estimated using the following formula: relative expression = $2^{-[C_T(\text{target gene}) - C_T(\text{GAPDH})]}$. The primers were designed as follows: *GAPDH*, 5'-ACCACAGTCCATGCCATCAC-3' (forward) and 5'-TCC-ACCCTGTTGCTGTA-3' (reverse); *CCL1*, 5'-GGAA-GAT-GTGGACAGCAAGAGC-3' (forward) and 5'-TGTA-GGG-CTGGTAGTTTCGG-3' (reverse); and *CCR8*, 5'-GTGTG-ACAACAGTGACCGACT-3' (forward) and 5'-CTT-CTTG-CAGACCACAAGGAC-3' (reverse).

Western Blot Analysis

Cells were lysed on ice using RIPA Lysis and Extraction Buffer (Thermo Fisher Scientific, Waltham, MA) containing 1% protease inhibitor and 1% phosphatase inhibitor cocktail (Sigma-Aldrich). The resulting lysates were separated onto 5% to 20% SDS polyacrylamide gels and transferred to a membrane using iBlot Gel Transfer Stack (Invitrogen, Carlsbad, CA). The membrane was blocked with 5% skim milk and incubated with primary and secondary antibodies.

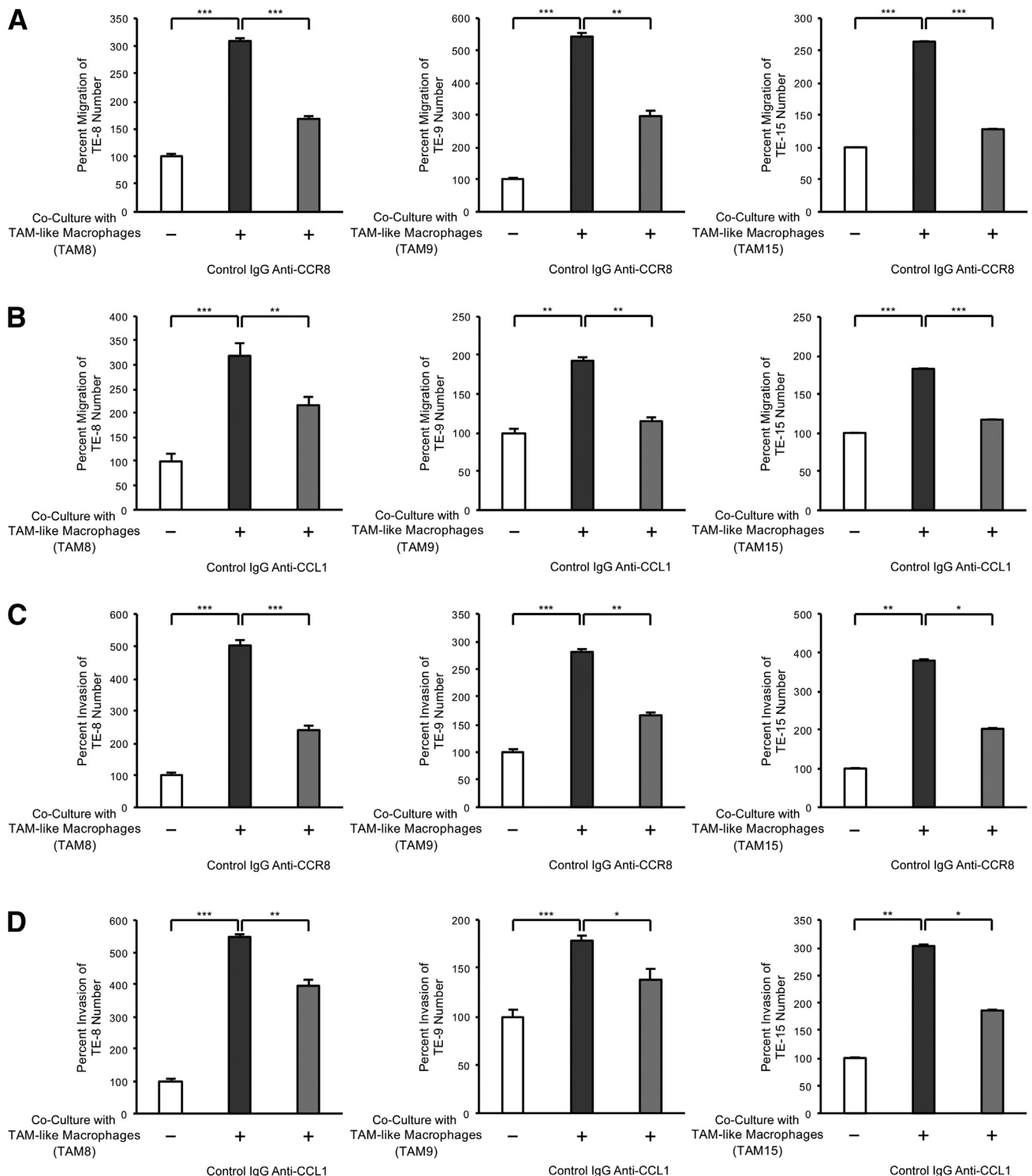
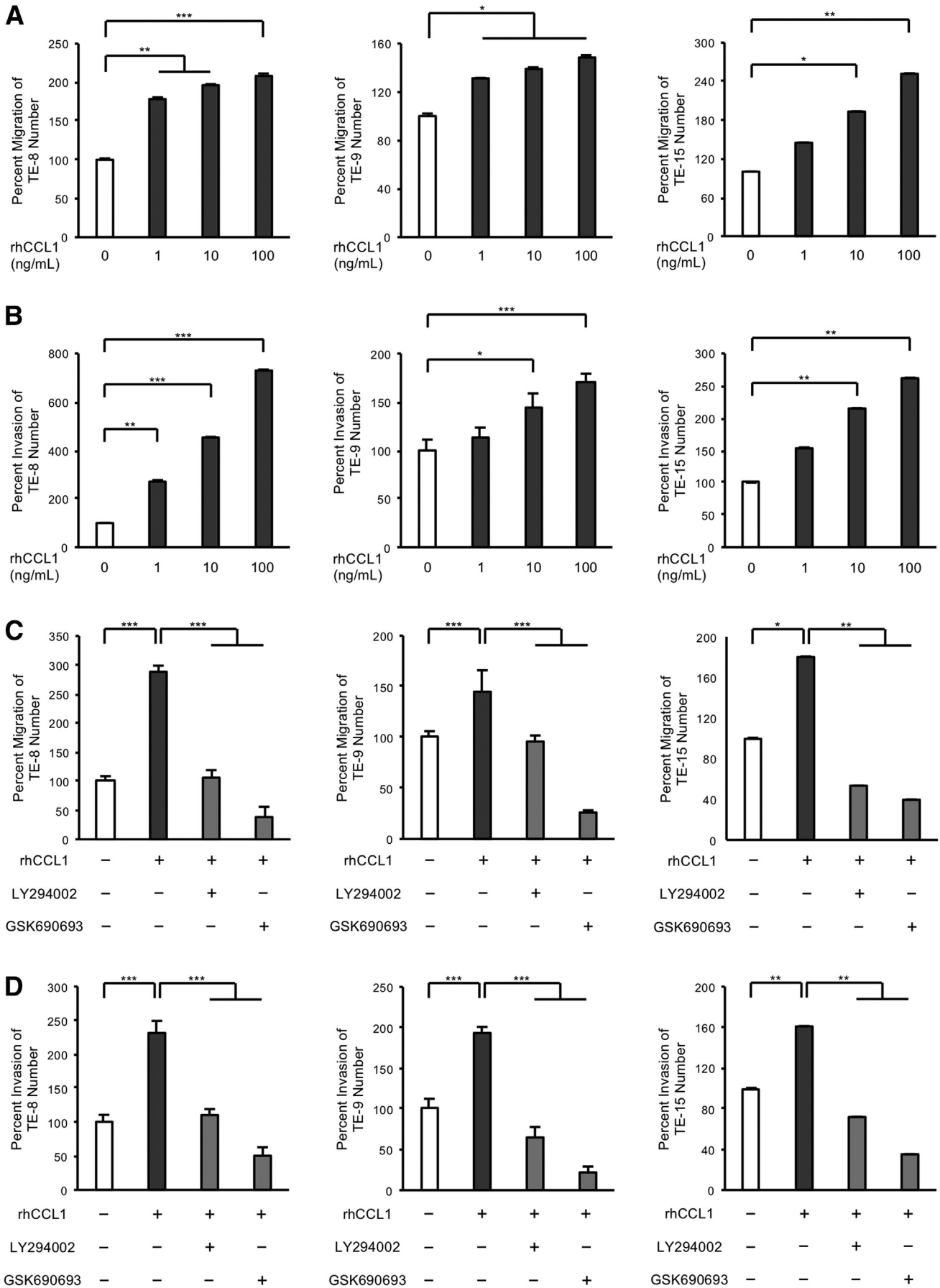


Figure 3 Chemokine (C-C motif) ligand 1 (CCL1), secreted by tumor-associated macrophage (TAM)-like macrophages, promoted TE-8, TE-9, and TE-15 cell migration and invasion. Transwell migration and invasion assays were performed to confirm the effect of neutralizing antibodies against CCL1 or CCR8 on co-culturing TE-8, TE-9, or TE-15 cells with TAM-like macrophages (TAM8, TAM9, or TAM15, respectively). **A:** Cells in the upper chamber were treated with a neutralizing antibody against CCR8 (anti-CCR8; 10 ng/mL) or rat IgG (10 ng/mL; control IgG; negative control); migrated cells were counted after 24 hours. **B:** Neutralizing antibody against CCL1 (anti-CCL1; 0.2 μ g/mL) or mouse IgG (0.2 μ g/mL; control IgG; negative control) was added to the lower chamber; migrated cells were counted after 24 hours. **C:** Cells in the upper chamber were treated with anti-CCR8 (10 ng/mL) or rat IgG (10 ng/mL; control IgG; negative control); invaded cells were counted after 48 hours. **D:** Anti-CCL1 (0.2 μ g/mL) or mouse IgG (0.2 μ g/mL; control IgG; negative control) was added to the lower chamber; invaded cells were counted after 48 hours. Results are expressed as means \pm SEM (**A–D**). * P < 0.05, ** P < 0.01, and *** P < 0.001.



The protein bands were detected with ImmunoStar Reagents (Wako).

The following primary antibodies were used: rabbit antibody against CCR8 (1:300; number ab8019; Abcam, Cambridge, UK), rabbit antibody against Akt (1:500; number 9272; Cell Signaling Technology, Beverly, MA), rabbit antibody against phosphorylated Akt (Ser473; 1:300; number 4060; Cell Signaling Technology), rabbit antibody against phosphorylated Akt (Thr308; 1:300; number 2965; Cell Signaling Technology), rabbit antibody against proline-rich Akt substrate of 40 kDa (PRAS40; 1:500; number 2961; Cell Signaling Technology), rabbit antibody against phosphorylated PRAS40 (Thr246; 1:300; number 13175; Cell Signaling Technology), rabbit antibody against mammalian target of rapamycin (mTOR; 1:200; number 2972; Cell Signaling Technology), rabbit antibody against phosphorylated mTOR (Ser2448; 1:200; number 2971; Cell Signaling Technology), and rabbit antibody against β -actin (1:1000; number 4970; Cell Signaling Technology). Horseradish peroxidase-linked donkey anti-rabbit IgG (number NA934V; GE Healthcare Life Science, Little Chalfont, UK) was used as the secondary antibody.

Survival and Growth Assay

TE-8, TE-9, or TE-15 cells were seeded in 96-well plates at a density of 1×10^4 cells per well and cultured in serum-free RPMI 1640 medium for the survival assay. Cells were seeded at a density of 5×10^3 cells per well and cultured in 1% FBS at 37°C for the growth assay. They were treated with 0 or 10 ng/mL recombinant human CCL1 (rhCCL1; R&D Systems). After 0, 24, 48, or 96 hours, CellTiter 96 Aqueous One Solution Reagent (Promega, Madison, WI) was added. Absorbance was measured using a microplate reader (Infinite 200 PRO; Tecan, Mannedorf, Switzerland) at 492 nm.

Transwell Migration and Invasion Assays

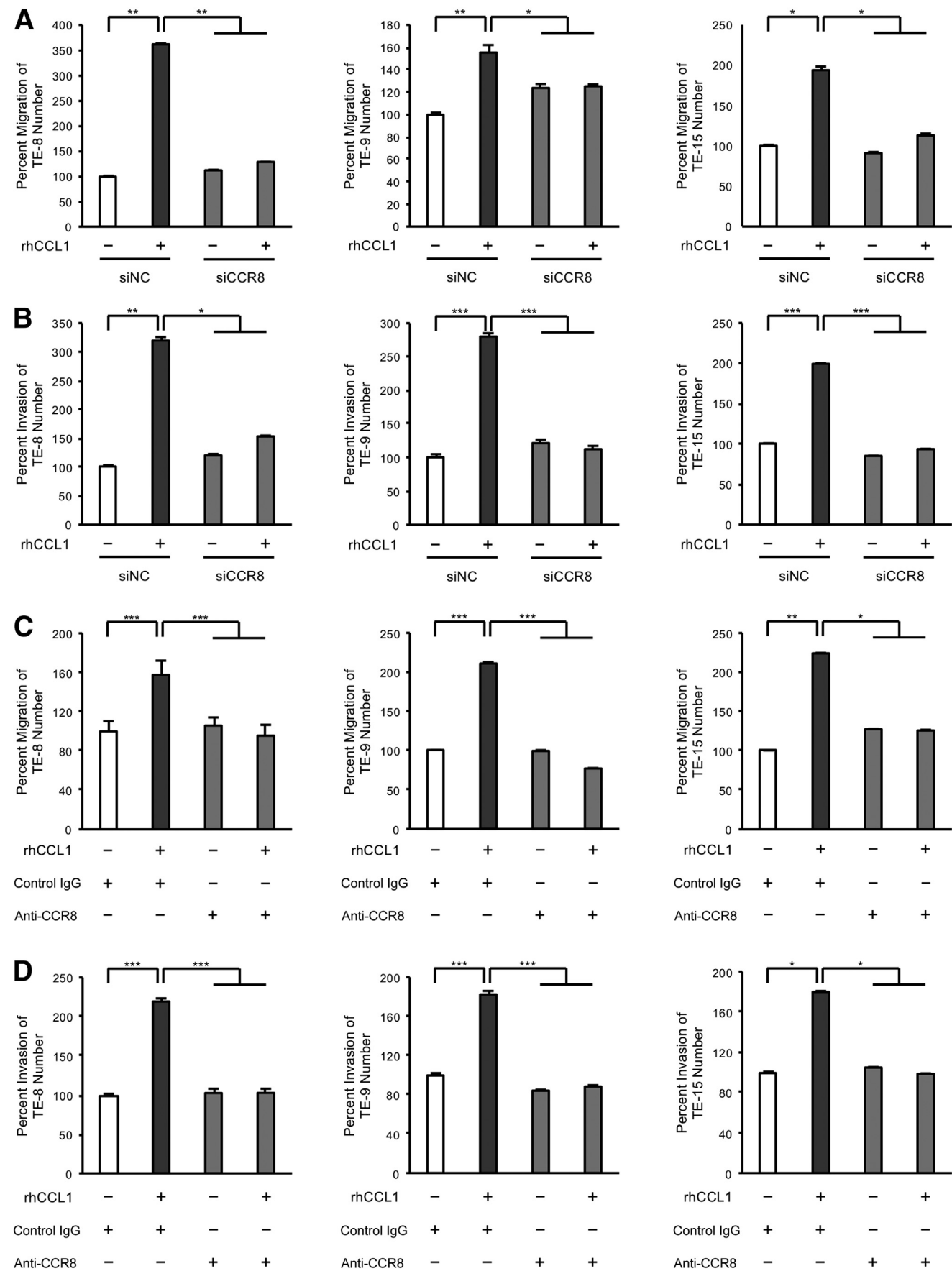
For the migration assay, TE-8, TE-9, or TE-15 cells (1×10^5 cells per well) in RPMI 1640 medium supplemented with 0.1% FBS were seeded in the upper chamber containing an

8- μ m pore filter (BD Falcon, Lincoln Park, NY) in 24-well plates. For the invasion assay, TE-8, TE-9, or TE-15 cells (2×10^5 cells per well) in RPMI 1640 medium supplemented with 0.1% FBS were seeded in the upper chamber of the Corning BioCoat Matrigel Invasion Chamber (Corning, Tewksbury, MA) in 24-well plates. RPMI 1640 medium containing 0.1% FBS was added to the lower chamber. Cells in the upper chamber were treated with phosphatidylinositol 3-kinase inhibitor (LY294002; 1 μ mol/L; Abcam), Akt inhibitor (GSK690693; 1 μ mol/L; Sigma-Aldrich), or neutralizing antibody against CCR8 (10 ng/mL). rhCCL1 (10 ng/mL) or a neutralizing antibody against CCL1 (0.2 μ g/mL) was added to the media in the lower chamber. After incubation at 37°C in a CO₂ incubator for 24 hours (migration assay) or 48 hours (invasion assay), the cells remaining on the surface of the membrane in the upper chamber were removed using a cotton swab. Cells on the lower surface of the membrane were stained using the Diff-Quik Kit (Sysmex, Kobe, Japan). Four images at $\times 100$ magnification were obtained from each membrane using a charge-coupled device camera, and cells were counted. The following neutralizing antibodies were used: mouse antibody against CCL1 (number MAB272; R&D Systems) and rat antibody against CCR8 (number MAB1429; R&D Systems); the following antibodies were used as the negative control: normal mouse IgG (number ab188776; Abcam) and normal rat IgG (number MAB0061; R&D Systems), respectively.

Co-Culture Transwell Migration and Invasion Assays

PBMos (1×10^5 cells per well) were seeded in the lower chamber in 24-well plates, and stimulated using macrophage colony-stimulating factor (25 ng/mL; R&D Systems) for six days to induce the formation of macrophages, followed by incubation with 50% CM of TE-8, TE-9, and TE-15 cells to induce the formation of TAM-like macrophages. After two days, the media were replaced with RPMI 1640 medium containing 0.1% FBS. TE-8, TE-9, or TE-15 cells (migration assay, 1×10^5 cells per well; invasion assay, 2×10^5 cells per well) in RPMI 1640 medium supplemented with 0.1% FBS were seeded in the upper chamber. Transwell migration and invasion assays were performed as described above.

Figure 4 Chemokine (C-C motif) ligand 1 (CCL1) promoted TE-8, TE-9, and TE-15 cell migration and invasion via the Akt/proline-rich Akt substrate of 40 kDa (PRAS40)/mammalian target of rapamycin (mTOR) signaling pathway. Migration and invasion assays were performed to evaluate the effect of the CCL1-CCR8 axis—via the Akt/PRAS40/mTOR signaling pathway—on the phenotypes of TE-8, TE-9, and TE-15 cells. **A:** TE-8, TE-9, and TE-15 cells in RPMI 1640 medium supplemented with 0.1% fetal bovine serum (FBS) were seeded in the upper chamber (1×10^5 cells per well). Recombinant human CCL1 (rhCCL1; 1, 10, and 100 ng/mL) was added to the lower chamber containing RPMI 1640 medium supplemented with 0.1% FBS; migrated cells were counted after 24 hours. **B:** TE-8, TE-9, and TE-15 cells in RPMI 1640 medium supplemented with 0.1% FBS were seeded in the Matrigel-coated upper chamber (2×10^5 cells per well). rhCCL1 (at 1, 10, and 100 ng/mL) was added to the lower chamber containing RPMI 1640 medium supplemented with 0.1% FBS; invaded cells were counted after 48 hours. **C:** TE-8, TE-9, and TE-15 cells in RPMI 1640 medium with 0.1% FBS were seeded in the upper chamber (1×10^5 cells per well). rhCCL1 (10 ng/mL), the negative control dimethyl sulfoxide (DMSO), an inhibitor of phosphatidylinositol 3-kinase (PI3K; LY294002; 1 μ mol/L), or an inhibitor of Akt (GSK690693; 1 μ mol/L) was added to the lower chamber containing RPMI 1640 medium supplemented with 0.1% FBS; migrated cells were counted after 24 hours. **D:** TE-8, TE-9, and TE-15 cells in RPMI 1640 medium with 0.1% FBS were seeded in the Matrigel-coated upper chamber (2×10^5 cells per well). rhCCL1 (10 ng/mL), a negative control DMSO, an inhibitor of PI3K (LY294002; 1 μ mol/L), or an inhibitor of Akt (GSK690693; 1 μ mol/L) was added to the lower chamber containing RPMI 1640 medium supplemented with 0.1% FBS; invaded cells were counted after 48 hours. Results are expressed as means \pm SEM (**A–D**). * $P < 0.05$, ** $P < 0.01$, and *** $P < 0.001$.



Enzyme-Linked Immunosorbent Assay

PBMo-derived macrophages, TAM-like macrophages, and TE-8, TE-9, and TE-15 cells were cultured in 6-well plates (5×10^5 cells per well) using RPMI 1640 medium containing 10% FBS. After 48 hours, the supernatants were harvested, and CCL1 levels were determined using the Human I-309 ELISA Kit (CCL1) (number ab100536; Abcam), according to the manufacturer's instructions. The OD of each well was measured using the Infinite 200 PRO Microplate Reader at 492 nm. The CCL1 concentration in each sample was calculated using a standard curve.

Phospho-Kinase Array

TE-8 cells were seeded in 60-mm dishes (5×10^5 cells per dish), and cultured in serum-free RPMI 1640 medium. After 24 hours, cells were incubated with or without rhCCL1 (10 ng/mL) for 10 minutes, and harvested for protein extraction. The proteins were analyzed using the Proteome Profiler Human Phospho-Kinase Array Kit (ARY003B; R&D Systems), according to the manufacturer's instructions.

CCR8 Knockdown Using siRNA

TE-8, TE-9, and TE-15 cells were transfected with 20 nmol/L siRNAs targeting *CCR8* (siCCR8; Sigma-Aldrich) using Lipofectamine RNAiMAX (Invitrogen). Cells transfected with control siRNA (siNC; Sigma-Aldrich) were used as the negative control.

Immunohistochemistry

Immunohistochemistry was performed using EnVision Dual Link System-HRP and 3,3'-diaminobenzidine (Dako Cytomation, Glostrup, Denmark). The following antibodies were used for antigen detection in ESCC tissues: rabbit antibody against CCL1 (1:50; number HPA049861; Atlas Antibody, Stockholm, Sweden) and rabbit antibody against CCR8 (1:100; number NBP2-15768; Novus Biologicals, Littleton, CO).

CCL1 expression in the stroma around the cancer nest was investigated at a magnification of $\times 100$ (four images) using a charge-coupled device camera, and CCL1-positive

stromal cells were counted. The median cell counts in the cancer stroma were obtained and samples were stratified into two groups (low and high).

CCR8 expression in the cancer nest was evaluated, and samples were stratified into two groups (negative and positive) based on the presence or absence of CCR8-positive cancer cells in the cancer nest.

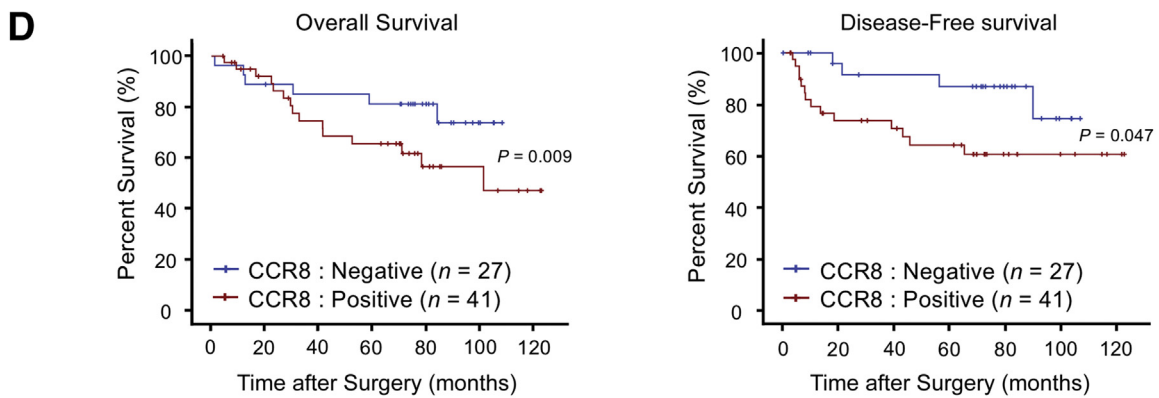
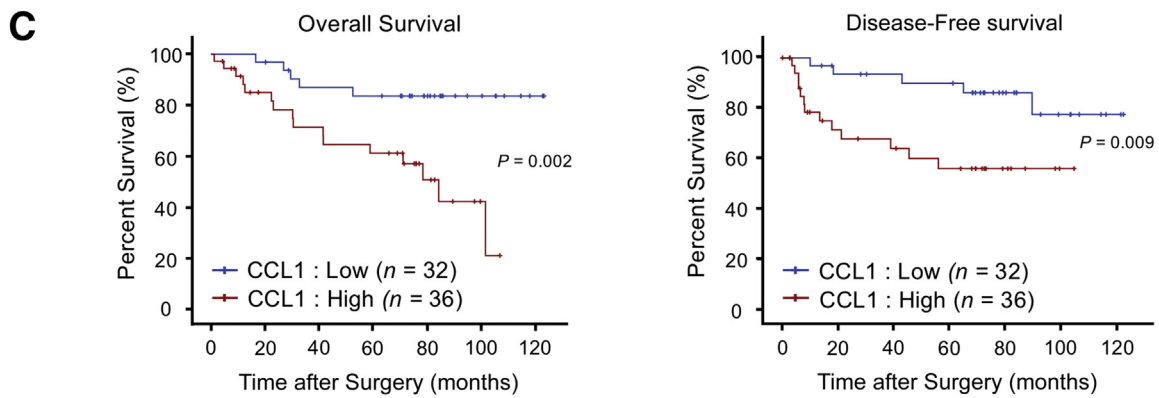
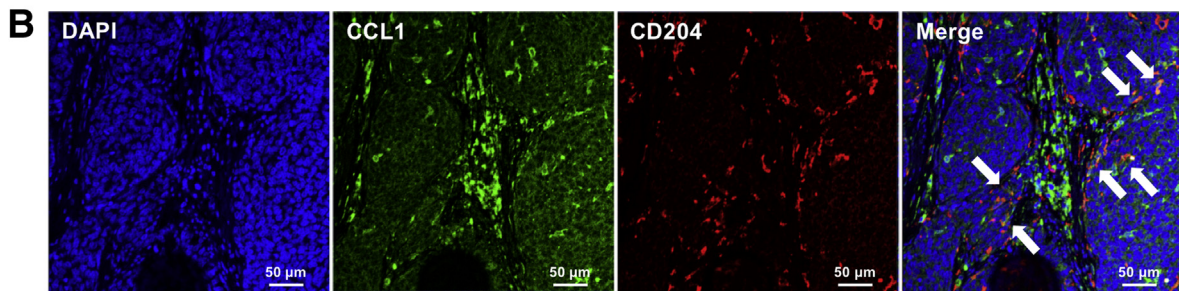
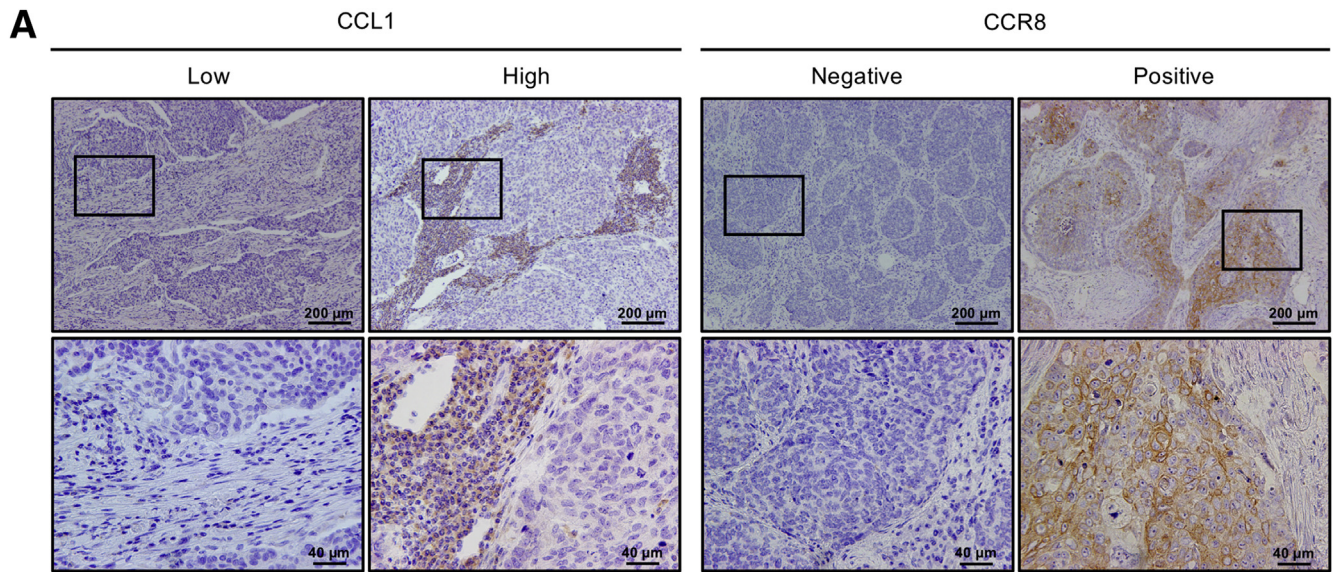
Immunofluorescence

PBMo-derived macrophages, TAM-like macrophages, and TE-8, TE-9, and TE-15 cells were seeded on coverslips, and fixed with 4% paraformaldehyde in phosphate buffer solution (Wako). PBMo-derived macrophages and TAM-like macrophages were incubated with rabbit antibody against CCL1 (1:50; number HPA049861; Atlas Antibody) and mouse antibody against CD204 (1:100; number KT022; Trans Genic Inc., Fukuoka, Japan) at 4°C overnight. ESCC tissues were incubated with rabbit antibody against CCL1 (1:50; number HPA049861; Atlas Antibody)/CCR8 (1:100; number NBP2-15768; Novus Biologicals), mouse antibody against CD204 (1:100; number KT022; Trans Genic Inc.), mouse antibody against forkhead box P3 (1:100; number 20034; Abcam), or sheep antibody against fibroblast activation protein (1:100; number AF3715; R&D systems) at 4°C overnight. TE-8, TE-9, and TE-15 cells were incubated with rabbit antibody against CCR8 (1:100; number ab32399; Abcam) at 4°C overnight. Cells that had been incubated with the primary antibodies were then incubated with Alexa Fluor 488—conjugated donkey anti-rabbit or sheep secondary antibody (1:200; Jackson ImmunoResearch Laboratories, West Grove, PA) and Cy3-conjugated donkey anti-mouse or rabbit secondary antibody (1:200; Jackson ImmunoResearch Laboratories) at room temperature for 1 hour. Nuclei were stained with DAPI (1:1000; number GV039; Wako). Images were obtained using the Zeiss LSM 700 laser-scanning microscope and analyzed using LSM ZEN 2009 (Carl Zeiss, Oberkochen, Germany).

Statistical Analysis

All *in vitro* experiments were performed in triplicate and were independently repeated three times. The results are expressed as means \pm SEM. Significance was analyzed using two-sided

Figure 5 siRNA against CCR8 (siCCR8) and neutralizing antibody against CCR8 (anti-CCR8) canceled the effects of recombinant human chemokine (C-C motif) ligand 1 (rhCCL1) on the phenotypes of the TE-8, TE-9, and TE-15 cells. **A:** TE-8, TE-9, or TE-15 cells, in RPMI 1640 medium supplemented with 0.1% fetal bovine serum (FBS), transfected with siCCR8 (20 nmol/L) or negative control siRNA (siNC; 20 nmol/L), were seeded in the upper chamber (1×10^5 cells per well). rhCCL1 (10 ng/mL) was added to the lower chamber containing RPMI 1640 medium supplemented with 0.1% FBS; migrated cells were counted after 24 hours. **B:** TE-8, TE-9, or TE-15 cells, in RPMI 1640 medium supplemented with 0.1% FBS, transfected with siCCR8 (20 nmol/L) or siNC (20 nmol/L) were seeded in the Matrigel-coated upper chamber (2×10^5 cells per well). rhCCL1 (10 ng/mL) was added to the lower chamber containing RPMI 1640 medium supplemented with 0.1% FBS; invaded cells were counted after 48 hours. **C:** TE-8, TE-9, or TE-15 cells, in RPMI 1640 medium supplemented with 0.1% FBS, were seeded in the upper chamber (1×10^5 cells per well) and treated with anti-CCR8 (10 ng/mL) or rat IgG (10 ng/mL; control IgG; negative control). rhCCL1 (10 ng/mL) was added to the lower chamber containing RPMI 1640 medium supplemented with 0.1% FBS; migrated cells were counted after 24 hours. **D:** TE-8, TE-9, or TE-15 cells, in RPMI 1640 medium supplemented with 0.1% FBS, were seeded in the upper chamber coated with Matrigel (2×10^5 cells per well) and treated with anti-CCR8 (10 ng/mL) or rat IgG (10 ng/mL; control IgG; negative control). rhCCL1 (10 ng/mL) was added to the lower chamber containing supplemented RPMI 1640 medium with 0.1% FBS; invaded cells were counted after 48 hours. Results are expressed as means \pm SEM (**A–D**). * $P < 0.05$, ** $P < 0.01$, and *** $P < 0.001$.



t-tests and Tukey-Kramer tests for comparing more than two groups. The relationships between clinicopathologic factors and immunohistochemical results were estimated using the χ^2 test. Kaplan-Meier curves were used to evaluate OS and disease-free survival, which were compared using log-rank tests. The significance of parameters in the univariate and multivariate analyses was evaluated using the Cox proportional hazard regression model. $P < 0.05$ was considered significant. Statistical analyses were performed using SPSS Statistics version 22 (IBM, Chicago, IL).

Results

CCL1 Expression Is Up-Regulated in TAM-Like Macrophages at the mRNA and Protein Level

First, up-regulation of CCL1 in TAM-like macrophages was confirmed. The expression of *CCL1* mRNA significantly increased on stimulation with CM from TE-8, TE-9, and TE-15 cells (relative to that in PBMo-derived macrophages). The expression of *CCL1* mRNA in TE-8, TE-9, and TE-15 cells was lower than that in PBMo-derived macrophages (Figure 1A). The concentration of secreted CCL1 was higher in TAM-like macrophages stimulated using CM of TE-8, TE-9, and TE-15 cells (TAM8, TAM9, and TAM15, in that order) than that in PBMo-derived macrophages (Figure 1B). CCL1 secretion from TE-8, TE-9, and TE-15 cells was undetectable (Figure 1B). Immunofluorescence also showed that CCL1 expression was higher in the cytoplasm of TAM-like macrophages than that in PBMo-derived macrophages (Figure 1C). These results suggest that CCL1 is expressed in TAM-like macrophages and is secreted.

CCL1 Activates the Akt/PRAS40/mTOR Signaling Pathway via CCR8 in TE-8, TE-9, and TE-15 Cells

RT-PCR and Western blot analysis confirmed the expression of CCR8—a CCL1 receptor—on TE-8, TE-9, and TE-15 cells (Figure 2, A and B). Immunofluorescence indicated CCR8 expression on cell membranes and in the cytoplasm of TE-8, TE-9, and TE-15 cells (Figure 2C).

Exploration of the CCL1-induced cell signaling pathway in TE-8 cells indicated that phosphorylated PRAS40 levels in rhCCL1 (10 ng/mL)—stimulated TE-8 cells were higher than those in the control (Figure 2D and Table 1). PRAS40 (ie, proline-rich Akt substrate of 40 kDa) is a substrate of Akt and a component of mammalian target of rapamycin complex 1.

As PRAS40 is involved in both the phosphatidylinositol 3-kinase/Akt signaling pathway and the mTOR signaling pathway, changes in the phosphorylation of Akt (Ser473 and Thr308), PRAS40 (Thr246), and mTOR (Ser2448) in TE-8, TE-9, and TE-15 cells were evaluated after rhCCL1 (10 ng/mL) stimulation using Western blot analysis (Figure 2E).

To further investigate the signaling pathway activated by the CCL1-CCR8 axis, TE-8, TE-9, and TE-15 cells were transfected using 20 nmol/L siCCR8 or siNC. CCR8 expression was lower in siCCR8-transfected TE-8, TE-9, and TE-15 cells than that in siNC-transfected TE-8, TE-9, and TE-15 cells as indicated by RT-PCR and Western blot analysis (Figure 2F). Next, siCCR8- or siNC-transfected TE-8, TE-9, and TE-15 cells were stimulated using rhCCL1 (10 ng/mL). Western blot analysis revealed that the levels of phosphorylated Akt (Ser473 and Thr308), PRAS40 (Thr246), and mTOR (Ser2448) after 10 minutes of stimulation were lower in siCCR8-transfected TE-8, TE-9, and TE-15 cells than those in siNC-transfected TE-8, TE-9, and TE-15 cells (Figure 2G). These results indicate that CCL1 activates the Akt/PRAS40/mTOR signaling pathway in ESCC cells via CCR8.

TAM-Like Macrophages Promote the Migration and Invasion of TE-8, TE-9, and TE-15 Cells via the CCL1-CCR8 Axis

To evaluate whether TAM-like macrophages promote malignant ESCC cell phenotypes, these cells were co-cultured using Transwell migration and invasion assays. TAM-like macrophages (TAM8, TAM9, and TAM15) significantly promoted the migration and invasion of TE-8, TE-9, and TE-15 cells, respectively (Figure 3). To investigate the role of the CCL1-CCR8 axis in regulating the effects of TAM-like macrophages (TAM8, TAM9, and TAM15) on TE-8, TE-9, and TE-15 cells, cells in the upper chamber were incubated with a neutralizing antibody against CCR8 or a neutralizing antibody against CCL1 was added to the lower chamber of the Transwell plate. Neutralizing antibodies against CCL1 and CCR8 significantly suppressed the migration and invasion of TAM-like macrophage (TAM8, TAM9, and TAM15)—stimulated TE-8, TE-9, and TE-15 cells, respectively (Figure 3). These results demonstrate that TAM-like macrophages promote the migration and invasion of ESCC cells via the CCL1-CCR8 axis.

Migration and Invasion of TE-8, TE-9, and TE-15 Cells Is Enhanced in Response to the Interaction between

Figure 6 High expression of chemokine (C-C motif) ligand 1 (CCL1) or CCR8 in human esophageal squamous cell carcinoma (ESCC) tissues was associated with a poor prognosis in ESCC patients. **A:** Immunohistochemistry was performed to check the expression of CCL1 or CCR8 in 69 human ESCC tissue samples. CCL1 expression was stratified as low intensity (Low) or high intensity (High), and CCR8 expression was stratified as negative immunoreaction (Negative) and positive immunoreaction (Positive). **Boxed areas** in the are shown at higher magnification in the **bottom ro**. **B:** Double immunofluorescence was performed using anti-CCL1 (green) and anti-CD204 (red) antibodies in human ESCC tissues. CD204-positive cells among CCL1-positive cells are shown in yellow (**arrows**). Nuclei were stained with DAPI (blue). Kaplan-Meier analysis of overall survival and disease-free survival with respect to CCL1 or CCR8 expression. **C:** Kaplan-Meier analysis of overall survival and disease-free survival in ESCC patients stratified into two groups (Low and High) based on the median values of CCL1-positive cells in the cancer stroma. **D:** Kaplan-Meier analysis of overall survival and disease-free survival in ESCC patients stratified into two groups (Negative and Positive) based on the presence of CCR8-positive cells in the cancer nest. Scale bars: 200 μ m (**A, top row**); 40 μ m (**A, bottom row**); 50 μ m (**B**).

CCL1 and CCR8 via the Akt/PRAS40/mTOR Signaling Pathway

rhCCL1 significantly accelerated the migration and invasion of TE-8, TE-9, and TE-15 cells in a concentration-dependent manner (Figure 4, A and B). The phosphatidylinositol 3-kinase inhibitor (LY294002) or Akt inhibitor (GSK690693) significantly inhibited the rhCCL1-induced enhancement of TE-8, TE-9, and TE-15 cell migration and invasion (Figure 4, C and D). Moreover, siCCR8 and the neutralizing antibody against CCR8 significantly suppressed the rhCCL1-induced increases in the migration and invasion of TE-8, TE-9, and TE-15 cells (Figure 5). These results suggest that the CCL1-CCR8 axis promotes TE-8, TE-9, and TE-15 cell migration and invasion via the Akt/PRAS40/mTOR signaling pathway. rhCCL1 does not affect TE-8, TE-9, and TE-15 cell proliferation and survival (Supplemental Figure S1).

CCL1 Expression Closely Correlates with Clinicopathologic Factors and Prognosis in ESCC

The expression of CCL1 and CCR8 was evaluated in human ESCC tissue samples using immunohistochemistry. ESCC patients ($n = 69$) were stratified on the basis of the median CCL1-positive cell counts into two groups (low and high) (Figure 6A). The patients were also stratified on the basis of the presence of CCR8-positive cells in the cancer nest, into two groups (negative and positive) (Figure 6A).

CCL1 was expressed in a portion of TAMs in ESCC tissues, as indicated by immunofluorescence (Figure 6B). CCL1 was expressed in TAMs as well as in other stromal cells, including forkhead box P3-positive Tregs and fibroblast activation protein-positive cancer-associated fibroblasts in ESCC tissues (Supplemental Figure S2, A and B). Immunofluorescence revealed that CCR8 was expressed in ESCC cells and in some Tregs and TAMs in ESCC tissues (Supplemental Figure S2, C and D).

Whether CCL1 or CCR8 expression is associated with clinicopathologic factors related to ESCC was investigated. CCL1 overexpression closely correlated with the depth of tumor invasion ($P = 0.002$), venous invasion ($P = 0.027$), CD68-positive macrophage counts ($P < 0.001$), CD163-positive macrophage counts ($P < 0.001$), and CD204-positive macrophage counts ($P < 0.001$) (Table 2). CCR8 positivity in the cancer nest closely correlated with the depth of tumor invasion ($P = 0.003$), lymphatic invasion ($P = 0.001$), stage ($P = 0.024$), and CD204-positive macrophage counts ($P = 0.011$) (Table 2).

Prognosis was evaluated using follow-up data from 68 of the 69 ESCC patients (excluding a single patient without follow-up data). Kaplan-Meier analysis revealed that patients in the CCL1-overexpression group had a significantly shorter OS ($P = 0.002$) and disease-free survival than those in the low CCL1 group ($P = 0.009$) (Figure 6C). Patients in the CCR8-positive group also had a significantly shorter OS ($P = 0.009$) and disease-free survival than those in the CCR8-negative

group ($P = 0.047$) (Figure 6D). Univariate Cox regression analysis of the prognostic factors revealed that a poor OS was closely correlated with the depth of tumor invasion [$P = 0.016$; hazard ratio (HR), 2.934; 95% CI, 1.225–7.025], lymphatic invasion ($P = 0.018$; HR, 2.924; 95% CI, 1.203–7.103), venous invasion ($P = 0.013$; HR, 3.079; 95% CI, 1.271–7.462), and CCL1 overexpression ($P = 0.005$; HR, 4.326; 95% CI, 1.569–11.927) (Table 3). Multivariate Cox regression analysis revealed that CCL1 overexpression was a significant independent predictive factor for poor OS in ESCC ($P = 0.016$; HR, 5.855; 95% CI, 1.393–24.620) (Table 3). These findings suggest that the CCL1-CCR8 axis in the tumor microenvironment contributes to a poor prognosis in patients with ESCC.

Discussion

In the present study, higher CCL1 levels were detected in ESCC cell CM-stimulated TAM-like macrophages than in PBMo-derived macrophages. CCL1 was not detected in the CM of ESCC cells. Wang et al⁴⁰ reported that CCL1 is secreted at significantly higher levels by programmed cell death-1-positive TAMs from gastric cancer tissues—which acquire tumor-progressive phenotypes and functional characteristics—than by programmed cell death-1-negative TAMs with tumor-suppressive phenotypes. Bladder and renal cancer tissues express high levels of CCL1; however, these cancer cell lines do not secrete detectable levels of CCL1.³⁶ Accordingly, CCL1 is thought to be secreted by cancer stromal cells, including TAMs.

CCR8 was expressed in the cell membrane and cytoplasm of ESCC cells. Although CCR8 is associated with various inflammatory diseases and Tregs in the cancer stroma, few studies have evaluated the association between CCR8-positive solid tumors and disease progression. Das et al³⁵ reported that CCL1, expressed by lymphatic endothelial cells, binds to CCR8, expressed on breast cancer and melanoma cells, and promotes tumor cell migration. Fu et al⁴¹ detected CCR8 expression on renal cell carcinoma cells using immunohistochemistry and showed that it is associated with poor prognosis. However, the signaling pathways mediating the effects of CCR8 in solid tumor cells have not been elucidated. Here, the role of PRAS40 was identified in the CCL1-CCR8 axis, which activated the Akt/PRAS40/mTOR signaling pathway in ESCC cells. The downstream effectors of the mTOR signaling pathway in tumor cells are reported to promote the cell migration and invasion via RhoA and Rac1 in colorectal cancer,⁴² and via S6K1 and 4E-BP1 in rhabdomyosarcoma⁴³ and various carcinomas.⁴⁴ In ESCC cells, the CCL1-CCR8 axis increased cell migration and invasion through the phosphatidylinositol 3-kinase/PRAS40/mTOR signaling pathway, possibly via similar downstream effectors. Other pathways in the CCL1-CCR8 axis have also been reported. For instance, Louahed et al⁴⁵ showed that the CCL1-CCR8 axis activates the

Table 2 CCL1 and CCR8 Expression Levels in Esophageal Squamous Cell Carcinoma and Their Correlations with Clinicopathologic Parameters and Infiltrating Macrophage Phenotypes

Variable	Expression of CCL1*				Expression of CCR8†			
	<i>n</i>	Low (<i>n</i> = 33)	High (<i>n</i> = 36)	<i>P</i> value	<i>n</i>	Negative (<i>n</i> = 28)	Positive (<i>n</i> = 41)	<i>P</i> value
Age, years								
<65	32	17	15	0.413	32	11	21	0.329
≥65	37	16	21		37	17	20	
Histologic grade‡								
HGIEN + WDSCC	15	7	8	0.919	15	6	9	0.959
MDSCC + PDSCC	54	26	28		54	22	32	
Depth of tumor invasion‡								
T1	48	29	19	0.002	48	25	23	0.003
T2 + T3	21	4	17		21	3	18	
Lymphatic invasion‡								
Negative	37	21	16	0.11	37	22	15	0.001
Positive	32	12	20		32	6	26	
Venous invasion‡								
Negative	43	25	18	0.027	43	20	23	0.197
Positive	26	8	18		26	8	18	
Lymph node metastasis‡								
Negative	43	24	19	0.088	43	21	22	0.554
Positive	26	9	17		26	7	19	
Stage§								
0 + I	38	22	16	0.064	38	20	18	0.024
II + III + IV	31	11	20		31	8	23	
CD68-positive cells¶								
Low	35	24	11	<0.001	35	15	20	0.696
High	34	9	25		34	13	21	
CD163-positive cells¶								
Low	34	27	7	<0.001	34	15	19	0.555
High	35	6	29		35	13	22	
CD204-positive cells¶								
Low	34	27	7	<0.001	34	19	15	0.011
High	35	6	29		35	9	26	

Data were analyzed using χ^2 test.

*Median values of CCL1-positive cells in cancer stroma were used to stratify the patients into two groups (low and high).

†CCR8 expression was used to stratify the patients into two groups (negative and positive) based on the presence of CCR8-positive cells in the cancer nest.

‡According to the Japanese Classification of Esophageal Cancer.³⁸

§According to the TNM classification by Union for International Cancer Control.³⁹

¶Median CD68-positive, CD163-positive, or CD204-positive macrophage counts in the cancer nests and stroma were used to stratify the patients into low and high groups.²¹

CCL1, chemokine (C-C motif) ligand 1; HGIEN, high-grade intraepithelial neoplasia; MDSCC, moderately differentiated squamous cell carcinoma; PDSCC, poorly differentiated squamous cell carcinoma; T1, tumor invades the mucosa (T1a) and the submucosa (T1b); T2, tumor invades the muscularis propria; T3, tumor invades the adventitia; WDSCC, well-differentiated squamous cell carcinoma.

anti-apoptotic activity in adult T-cell leukemia via the RAS/mitogen-activated protein kinase signaling pathway. Reipschläger et al⁴⁶ reported that the CCL1-CCR8 axis exerts its effects via the janus kinase/STAT signaling pathway in human embryonic kidney cells.

TAM-like macrophages significantly promoted the migration and invasion of ESCC cells in a co-culture Transwell assay. This result indicated the presence of paracrine interactions between TAM-like macrophages and ESCC cells. These effects were suppressed on using neutralizing antibodies against CCL1 and CCR8, indicating that the influence of CCL1-CCR8 axis on their paracrine interactions

partially contributes to the malignant phenotypes of ESCC cells. With regard to the paracrine interactions between TAM and ESCC, not only the CCL1-CCR8 axis, but several factors, such as growth differentiation factor 15,²² CXCL8-CXCR1/2 axis,²⁵ and CCL3-CCR5 axis,²⁶ also play an important role in promoting the malignancy of ESCC cells.

The promotion of cell motility by CCL1 has been reported in melanoma³⁵ and endothelial cells.⁴⁷ The Transwell assay revealed that the activation of the Akt/PRAS40/mTOR signaling pathway by the CCL1-CCR8 axis plays an important role in ESCC cell motility. However, the effects of CCL1 on the growth and survival

Table 3 Relationship between Clinicopathologic Parameters of Esophageal Squamous Cell Carcinoma and Overall Survival

Variable	Univariate analysis					Multivariate analysis		
	Median survival							
	<i>n</i>	Time, months	HR	95% CI	<i>P</i> value	HR	95% CI	<i>P</i> value
Age, years								
<65	32	97.613	1.61	0.668–3.881	0.289			
≥65	36	86.42						
Histological grade*								
HGIEN + WDSCC	15	72.052	0.922	0.334–2.547	0.876			
MDSCC + PDSCC	53	91.248						
Depth of tumor invasion*								
T1	48	98.826	2.934	1.225–7.025	0.016	1.103	0.350–3.477	0.867
T2 + T3	20	69.636						
Lymphatic invasion*								
Negative	37	102.38	2.924	1.203–7.103	0.018	2.145	0.633–7.261	0.22
Positive	31	76.115						
Venous invasion*								
Negative	43	101.005	3.079	1.271–7.462	0.013	1.854	0.642–5.358	0.254
Positive	25	60.795						
Lymph node metastasis*								
Negative	43	95.779	1.591	0.666–3.805	0.296			
Positive	25	75.92						
Stage†								
0 + I	38	97.966	1.919	0.805–4.571	0.141			
II + III + IV	30	75.083						
Expression of CCL1‡								
Low	32	108.113	4.326	1.569–11.927	0.005	5.855	1.393–24.620	0.016
High	36	68.708						
Expression of CCR8§								
Negative	27	90.586	2.086	0.805–5.405	0.13			
Positive	41	84.026						
CD68-positive cells¶								
Low	35	100.656	2.029	0.839–4.905	0.116			
High	33	78.19						
CD163-positive cells¶								
Low	34	101.478	2.36	0.949–5.864	0.065	0.47	0.119–1.849	0.28
High	34	79.995						
CD204-positive cells¶								
Low	34	99.538	1.995	0.825–4.822	0.125			
High	34	81.661						

Overall survival was estimated using the Kaplan-Meier method and compared by the log-rank test.

*According to the Japanese Classification of Esophageal Cancer.³⁸

†According to the TNM classification by Union for International Cancer Control.³⁹

‡Median values for CCL1-positive cells in the cancer stroma were used to stratify the patients into two groups (low and high).

§Patients were stratified into two groups (negative and positive) based on presence of CCR8-positive cells in the cancer nest.

¶Median CD68-positive, CD163-positive, or CD204-positive macrophage numbers in the cancer nests and stroma were used to stratify the patients into low and high groups.²¹

CCL1, chemokine (C-C motif) ligand 1; HGIEN, high-grade intraepithelial neoplasia; HR, hazard ratio; MDSCC, moderately differentiated squamous cell carcinoma; PDSCC, poorly differentiated squamous cell carcinoma; T1, tumor invades the mucosa (T1a) and the submucosa (T1b); T2, tumor invades the muscularis propria; T3, tumor invades the adventitia; WDSCC, well-differentiated squamous cell carcinoma.

of cancer cells are controversial. No effect of CCL1 on ESCC cell growth or survival was observed. In contrast, Denis et al⁴⁸ showed that CCL1 suppresses thymic lymphoma cell apoptosis. Cao et al⁴⁹ showed that high CCL1 expression inhibits apoptosis and promotes the proliferation of bladder cancer cells. In addition, CCL1 enhances the chemoresistance of colorectal cancer cells.⁵⁰ CCL1

might have different functions, depending on the origin and histologic type of cancer cells.

The immunohistochemical and immunofluorescence analyses in the current study indicate CCL1 expression in the cancer stroma and CCR8 expression in the cancer stroma and cancer nest in the ESCC tissues. CD204-positive TAMs as well as fibroblast activation protein–positive cancer-

associated fibroblasts and forkhead box P3—positive Tregs expressed CCL1 in the cancer stroma of ESCC tissues. Immunofluorescence revealed that CCR8 was mainly expressed in ESCC cells; however, some Tregs and TAMs also exhibited CCR8 positivity. CCL1 has been reported to be expressed by Snail-positive fibroblasts in colorectal cancer⁵⁰ and by fibroblasts co-cultured with bladder cancer cells.⁵¹ Kuehnemuth et al⁵² reported that the high CCL1 expression in breast cancer is significantly correlated with high infiltrating forkhead box P3—positive Treg counts. Wiedemann et al⁵³ demonstrated that CCL1 expression is significantly correlated with the number of cancer stromal cells, including Tregs, in hepatocellular cell carcinoma. These observations may indicate that CCL1 is secreted by stromal cells, including TAMs, cancer-associated fibroblasts, and Tregs. The CCL1-CCR8 axis is a part of an autocrine loop in Tregs.⁵⁴ In general, CCR8 is expressed on cancer stromal cells, including Tregs^{55–57} and TAMs,³⁶ in the tumor microenvironment. However, few studies have described the expression of CCR8 on cancer cells in tumor tissues. CCR8 expression has been confirmed by immunohistochemistry in glioblastoma,⁵⁸ renal cancer,⁴¹ melanoma, and breast cancer cells.³⁵ CCL1, secreted by cancer stromal cells, may affect tumor progression via CCR8 expressed on cancer cell surface *in vivo*.

Prior studies show that CCL1 overexpression in cancer tissue tends to be correlated with a poor prognosis in breast cancer.⁵² CCR8 expression in the cancer nest is associated with poor prognosis in glioblastoma⁵⁸ and renal cancer.⁴¹ However, the correlations between prognosis and the expression of CCL1 in the cancer stroma and CCR8 in the cancer nest have not been evaluated. Here, we confirmed the significant association between poor prognosis in ESCC and the overexpression of CCL1 in the cancer stroma or CCR8 in the cancer nest. CCL1 overexpression in the cancer stroma of patients with ESCC was a significant independent prognostic factor. However, the limitations of the present study lie in the clinicopathologic and prognosis analyses. The current analysis of the correlation between prognosis and CCL1 or CCR8 expression involved a limited number of patients. The sample size included in the study ($n = 69$) is considered small scale with regard to a prognosis analysis. Future studies with a larger sample size of ESCC tissues need to be designed to validate these findings and to confirm the prognostic significance of CCL1 or CCR8.

In conclusion, we demonstrate that CCL1 expression in cancer stromal cells, including TAMs, promotes tumor progression in ESCC and is associated with poor prognosis. These effects of CCL1 are mediated by CCR8—expressed on cancer cells—via the Akt/PRAS40/mTOR signaling pathway. The chemokine ligand/chemokine receptor axes play important roles in tumor-immune interactions; therefore, these axes serve as potential targets for tumor immunotherapy. However, another limitation of this study was that the effects of inhibition of the CCL1-CCR8 axis were not analyzed on the ESCC microenvironment *in vivo*. It is necessary to investigate the effects of CCL1-CCR8 axis

inhibition using neutralizing antibodies or specific inhibitors in severe combined immunodeficiency mouse xenograft models of ESCC cells in future studies. In oncological therapy, the effects of targeting the CCL1-CCR8 axis have not been investigated using clinical trials. Villarreal et al⁵⁹ recently reported that an anti-CCR8 antibody suppresses tumor progression in a mouse colorectal cancer model. Hoelzinger et al⁶⁰ reported that an anti-CCL1 antibody enhanced tumor immunotherapy via inhibition of Treg. The blockage of the CCL1-CCR8 axis using anti-CCL1 or anti-CCR8 antibodies could serve as a novel immune checkpoint therapy by regulating the recruitment of Tregs.^{61,62} Accordingly, the CCL1-CCR8 axis acting via the Akt/PRAS40/mTOR signaling pathway may serve as a prognostic marker and new therapeutic target in ESCC.

Acknowledgments

We thank Atsuko Kawashima, Yumi Hashimoto, Nobuo Kubo, and Miki Yamazaki for excellent technical support.

Supplemental Data

Supplemental material for this article can be found at <http://doi.org/10.1016/j.ajpath.2021.01.004>.

References

- Bray F, Ferlay J, Soerjomataram I, Siegel RL, Torre LA, Jemal A: Global cancer statistics 2018: GLOBOCAN estimates of incidence and mortality worldwide for 36 cancers in 185 countries. *CA Cancer J Clin* 2018, 68:394–424
- Tungekar A, Mandarathi S, Mandaviya PR, Gadekar VP, Tantry A, Kotian S, Reddy J, Prabha D, Bhat S, Sahay S, Mascarenhas R, Badkillaya RR, Nagasampige MK, Yelnadu M, Pawar H, Hebbar P, Kashyap MK: ESCC ATLAS: a population wide compendium of biomarkers for esophageal squamous cell carcinoma. *Sci Rep* 2018, 8:12715
- Abnet CC, Arnold M, Wei WQ: Epidemiology of esophageal squamous cell carcinoma. *Gastroenterology* 2018, 154:360–373
- Lagergren J, Smyth E, Cunningham D, Lagergren P: Oesophageal cancer. *Lancet* 2017, 390:2383–2396
- Gamliel Z, Krasna MJ: Multimodality treatment of esophageal cancer. *Surg Clin North Am* 2005, 85:621–630
- Wang Y, Zhu L, Xia W, Wang F: Anatomy of lymphatic drainage of the esophagus and lymph node metastasis of thoracic esophageal cancer. *Cancer Manag Res* 2018, 10:6295–6303
- Enzinger PC, Mayer RJ: Esophageal cancer. *N Engl J Med* 2003, 349:2241–2252
- Lin DC, Wang MR, Koeffler HP: Genomic and epigenomic aberrations in esophageal squamous cell carcinoma and implications for patients. *Gastroenterology* 2018, 154:374–389
- Li H, Fan X, Houghton J: Tumor microenvironment: the role of the tumor stroma in cancer. *J Cell Biochem* 2007, 101:805–815
- Lin EW, Karakasheva TA, Hicks PD, Bass AJ, Rustgi AK: The tumor microenvironment in esophageal cancer. *Oncogene* 2016, 35:5337–5349
- Yokozaki H, Koma YI, Shigeoka M, Nishio M: Cancer as a tissue: the significance of cancer-stromal interactions in the development,

- morphogenesis and progression of human upper digestive tract cancer. *Pathol Int* 2018, 68:334–352
12. Sica A, Schioppa T, Mantovani A, Allavena P: Tumour-associated macrophages are a distinct M2 polarised population promoting tumour progression: potential targets of anti-cancer therapy. *Eur J Cancer* 2006, 42:717–727
 13. Takeya M, Komohara Y: Role of tumor-associated macrophages in human malignancies: friend or foe? *Pathol Int* 2016, 66:491–505
 14. Komohara Y, Jinushi M, Takeya M: Clinical significance of macrophage heterogeneity in human malignant tumors. *Cancer Sci* 2014, 105:1–8
 15. Komohara Y, Ohnishi K, Kuratsu J, Takeya M: Possible involvement of the M2 anti-inflammatory macrophage phenotype in growth of human gliomas. *J Pathol* 2008, 216:15–24
 16. Binnemars-Postma K, Storm G, Prakash J: Nanomedicine strategies to target tumor-associated macrophages. *Int J Mol Sci* 2017, 18:979
 17. Ohtaki Y, Ishii G, Nagai K, Ashimine S, Kuwata T, Hishida T, Nishimura M, Yoshida J, Takeyoshi I, Ochiai A: Stromal macrophage expressing CD204 is associated with tumor aggressiveness in lung adenocarcinoma. *J Thorac Oncol* 2010, 5:1507–1515
 18. Zhang M, He Y, Sun X, Li Q, Wang W, Zhao A, Di W: A high M1/M2 ratio of tumor-associated macrophages is associated with extended survival in ovarian cancer patients. *J Ovarian Res* 2014, 7:19
 19. Wang B, Liu H, Dong X, Wu S, Zeng H, Liu Z, Wan D, Dong W, He W, Chen X, Zheng L, Huang J, Lin T: High CD204+ tumor-infiltrating macrophage density predicts a poor prognosis in patients with urothelial cell carcinoma of the bladder. *Oncotarget* 2015, 6:20204–20214
 20. Miyasato Y, Shiota T, Ohnishi K, Pan C, Yano H, Horlad H, Yamamoto Y, Yamamoto-Ibusuki M, Iwase H, Takeya M, Komohara Y: High density of CD204-positive macrophages predicts worse clinical prognosis in patients with breast cancer. *Cancer Sci* 2017, 108:1693–1700
 21. Shigeoka M, Urakawa N, Nakamura T, Nishio M, Watajima T, Kuroda D, Komori T, Kakeji Y, Semba S, Yokozaki H: Tumor associated macrophage expressing CD204 is associated with tumor aggressiveness of esophageal squamous cell carcinoma. *Cancer Sci* 2013, 104:1112–1119
 22. Urakawa N, Utsunomiya S, Nishio M, Shigeoka M, Takase N, Arai N, Kakeji Y, Koma YI, Yokozaki H: GDF15 derived from both tumor-associated macrophages and esophageal squamous cell carcinomas contributes to tumor progression via Akt and Erk pathways. *Lab Invest* 2015, 95:491–503
 23. Okamoto M, Koma YI, Kodama T, Nishio M, Shigeoka M, Yokozaki H: Growth differentiation factor 15 promotes progression of esophageal squamous cell carcinoma via TGF-beta type II receptor activation. *Pathobiology* 2020, 87:100–113
 24. Takase N, Koma YI, Urakawa N, Nishio M, Arai N, Akiyama H, Shigeoka M, Kakeji Y, Yokozaki H: NCAM- and FGF-2-mediated FGFR1 signaling in the tumor microenvironment of esophageal cancer regulates the survival and migration of tumor-associated macrophages and cancer cells. *Cancer Lett* 2016, 380:47–58
 25. Hosono M, Koma YI, Takase N, Urakawa N, Higashino N, Suemune K, Kodaira H, Nishio M, Shigeoka M, Kakeji Y, Yokozaki H: CXCL8 derived from tumor-associated macrophages and esophageal squamous cell carcinomas contributes to tumor progression by promoting migration and invasion of cancer cells. *Oncotarget* 2017, 8:106071–106088
 26. Kodama T, Koma YI, Arai N, Kido A, Urakawa N, Nishio M, Shigeoka M, Yokozaki H: CCL3-CCR5 axis contributes to progression of esophageal squamous cell carcinoma by promoting cell migration and invasion via Akt and ERK pathways. *Lab Invest* 2020, 100:1140–1157
 27. Miller MD, Wilson SD, Dorf ME, Seunanez HN, O'Brien SJ, Krangel MS: Sequence and chromosomal location of the I-309 gene: relationship to genes encoding a family of inflammatory cytokines. *J Immunol* 1990, 145:2737–2744
 28. Miller MD, Krangel MS: The human cytokine I-309 is a monocyte chemoattractant. *Proc Natl Acad Sci U S A* 1992, 89:2950–2954
 29. Tiffany HL, Lautens LL, Gao JL, Pease J, Locati M, Combadiere C, Modi W, Bonner TI, Murphy PM: Identification of CCR8: a human monocyte and thymus receptor for the CC chemokine I-309. *J Exp Med* 1997, 186:165–170
 30. de Munnik SM, Smit MJ, Leurs R, Vischer HF: Modulation of cellular signaling by herpesvirus-encoded G protein-coupled receptors. *Front Pharmacol* 2015, 6:40
 31. McCully ML, Moser B: The human cutaneous chemokine system. *Front Immunol* 2011, 2:33
 32. Yang R, Liao Y, Wang L, He P, Hu Y, Yuan D, Wu Z, Sun X: Exosomes derived from M2b macrophages attenuate DSS-induced colitis. *Front Immunol* 2019, 10:2346
 33. Montes-Vizuet R: CC chemokine ligand 1 is released into the airways of atopic asthmatics. *Eur Respir J* 2006, 28:59–67
 34. Gombert M, Dieu-Nosjean MC, Winterberg F, Bunemann E, Kubitz RC, Da Cunha L, Haahela A, Lehtimäki S, Müller A, Rieker J, Meller S, Pivarsci A, Koreck A, Fridman WH, Zentgraf HW, Pavenstadt H, Amara A, Caux C, Kemeny L, Alenius H, Lauerma A, Ruzicka T, Zlotnik A, Homey B: CCL1-CCR8 interactions: an axis mediating the recruitment of T cells and Langerhans-type dendritic cells to sites of atopic skin inflammation. *J Immunol* 2005, 174:5082–5091
 35. Das S, Sarrou E, Podgrabinska S, Cassella M, Mungamuri SK, Feirt N, Gordon R, Nagi CS, Wang Y, Entenberg D, Condeelis J, Skobe M: Tumor cell entry into the lymph node is controlled by CCL1 chemokine expressed by lymph node lymphatic sinuses. *J Exp Med* 2013, 210:1509–1528
 36. Eruslanov E, Stoffs T, Kim WJ, Daurkin I, Gilbert SM, Su LM, Vieweg J, Daaka Y, Kusmartsev S: Expansion of CCR8(+) inflammatory myeloid cells in cancer patients with urothelial and renal carcinomas. *Clin Cancer Res* 2013, 19:1670–1680
 37. Nishihira T, Hashimoto Y, Katayama M, Mori S, Kuroki T: Molecular and cellular features of esophageal cancer cells. *J Cancer Res Clin Oncol* 1993, 119:441–449
 38. Japan Esophageal Society: Japanese Classification of Esophageal Cancer. ed 10. Tokyo, Japan, Kanehara & Co, 2008
 39. Sobin LH, Gospodarowicz MK, Wittekind C (Eds): TNM Classification of Malignant Tumours. ed 7. Hoboken, NJ: Wiley-Blackwell, 2011
 40. Wang F, Li B, Wei Y, Zhao Y, Wang L, Zhang P, Yang J, He W, Chen H, Jiao Z, Li Y: Tumor-derived exosomes induce PD1(+) macrophage population in human gastric cancer that promotes disease progression. *Oncogenesis* 2018, 7:41
 41. Fu Q, Chang Y, Zhou L, An H, Zhu Y, Xu L, Zhang W, Xu J: Positive intratumoral chemokine (C-C motif) receptor 8 expression predicts high recurrence risk of post-operation clear-cell renal cell carcinoma patients. *Oncotarget* 2016, 7:8413–8421
 42. Gulhati P, Bowen KA, Liu J, Stevens PD, Rychahou PG, Chen M, Lee EY, Weiss HL, O'Connor KL, Gao T, Evers BM: mTORC1 and mTORC2 regulate EMT, motility, and metastasis of colorectal cancer via RhoA and Rac1 signaling pathways. *Cancer Res* 2011, 71:3246–3256
 43. Liu L, Li F, Cardelli JA, Martin KA, Blenis J, Huang S: Rapamycin inhibits cell motility by suppression of mTOR-mediated S6K1 and 4E-BP1 phosphorylation. *Oncogene* 2006, 25:7029–7040
 44. Zhou H, Huang S: Role of mTOR signaling in tumor cell motility, invasion and metastasis. *Curr Protein Pept Sci* 2011, 12:30–42
 45. Louahed J, Struyf S, Demoulin JB, Parmentier M, Van Snick J, Van Damme J, Renault JC: CCR8-dependent activation of the RAS/MAPK pathway mediates anti-apoptotic activity of I-309/CCL1 and vMIP-I. *Eur J Immunol* 2003, 33:494–501
 46. Reipschläger S, Kubatzky K, Taromi S, Burger M, Orth J, Aktories K, Schmidt G: Toxin-induced RhoA activity mediates CCL1-triggered signal transducers and activators of transcription protein signaling. *J Biol Chem* 2012, 287:11183–11194
 47. Bernardini G, Spinetti G, Ribatti D, Camarda G, Morbidelli L, Ziche M, Santoni A, Capogrossi MC, Napolitano M: I-309 binds to and activates endothelial cell functions and acts as an angiogenic molecule in vivo. *Blood* 2000, 96:4039–4045

48. Denis C, Deiteren K, Mortier A, Tounsi A, Fransen E, Proost P, Renaud JC, Lambeir AM: C-terminal clipping of chemokine CCL1/I-309 enhances CCR8-mediated intracellular calcium release and anti-apoptotic activity. *PLoS One* 2012, 7:e34199
49. Cao Q, Wang N, Qi J, Gu Z, Shen H: Long non-coding RNA-GAS5 acts as a tumor suppressor in bladder transitional cell carcinoma via regulation of chemokine (C-C motif) ligand 1 expression. *Mol Med Rep* 2016, 13:27–34
50. Li Z, Chan K, Qi Y, Lu L, Ning F, Wu M, Wang H, Wang Y, Cai S, Du J: Participation of CCL1 in snail-positive fibroblasts in colorectal cancer contribute to 5-fluorouracil/paclitaxel chemoresistance. *Cancer Res Treat* 2018, 50:894–907
51. Yeh CR, Hsu I, Song W, Chang H, Miyamoto H, Xiao GQ, Li L, Yeh S: Fibroblast ERalpha promotes bladder cancer invasion via increasing the CCL1 and IL-6 signals in the tumor microenvironment. *Am J Cancer Res* 2015, 5:1146–1157
52. Kuehnemuth B, Piseddu I, Wiedemann GM, Lauseker M, Kuhn C, Hofmann S, Schmoeckel E, Endres S, Mayr D, Jeschke U, Anz D: CCL1 is a major regulatory T cell attracting factor in human breast cancer. *BMC Cancer* 2018, 18:1278
53. Wiedemann GM, Rohrl N, Makeschin MC, Fessler J, Endres S, Mayr D, Anz D: Peritumoral CCL1 and CCL22 expressing cells in hepatocellular carcinomas shape the tumour immune infiltrate. *Pathology* 2019, 51:586–592
54. Barshesht Y, Wildbaum G, Levy E, Vitenshtein A, Akinseye C, Griggs J, Lira SA, Karin N: CCR8(+)FOXP3(+) Treg cells as master drivers of immune regulation. *Proc Natl Acad Sci U S A* 2017, 114: 6086–6091
55. Plitas G, Konopacki C, Wu K, Bos PD, Morrow M, Putintseva EV, Chudakov DM, Rudensky AY: Regulatory T cells exhibit distinct features in human breast cancer. *Immunity* 2016, 45:1122–1134
56. De Simone M, Arrighi A, Rossetti G, Gruarin P, Ranzani V, Politano C, Bonnal RJP, Provati E, Sarnicola ML, Panzeri I, Moro M, Crosti M, Mazzara S, Vaira V, Bosari S, Palleschi A, Santambrogio L, Bovo G, Zucchini N, Totis M, Gianotti L, Cesana G, Perego RA, Maroni N, Pisani Ceretti A, Opocher E, De Francesco R, Geginat J, Stunnenberg HG, Abbrignani S, Pagani M: Transcriptional landscape of human tissue lymphocytes unveils uniqueness of tumor-infiltrating T regulatory cells. *Immunity* 2016, 45:1135–1147
57. Wang L, Simons DL, Lu X, Tu TY, Solomon S, Wang R, Rosario A, Avalos C, Schmolze D, Yim J, Waisman J, Lee PP: Connecting blood and intratumoral Treg cell activity in predicting future relapse in breast cancer. *Nat Immunol* 2019, 20:1220–1230
58. Berenguer J, Lagerweij T, Zhao XW, Dusoswa S, van der Stoop P, Westerman B, de Gooijer MC, Zoetemelk M, Zomer A, Crommentuijn MHW, Wedekind LE, Lopez-Lopez A, Giovanazzi A, Bruch-Oms M, van der Meulen-Muileman IH, Reijmers RM, van Kuppevelt TH, Garcia-Vallejo JJ, van Kooyk Y, Tannous BA, Wesseling P, Koppers-Lalic D, Vandertop WP, Noske DP, van Beusechem VW, van Rheenen J, Pegtel DM, van Tellingen O, Wurdinger T: Glycosylated extracellular vesicles released by glioblastoma cells are decorated by CCL18 allowing for cellular uptake via chemokine receptor CCR8. *J Extracell Vesicles* 2018, 7: 1446660
59. Villarreal DO, L'Huillier A, Armington S, Mottershead C, Filippova EV, Coder BD, Petit RG, Princiotta MF: Targeting CCR8 induces protective antitumor immunity and enhances vaccine-induced responses in colon cancer. *Cancer Res* 2018, 78: 5340–5348
60. Hoelzinger DB, Smith SE, Mirza N, Dominguez AL, Manrique SZ, Lustgarten J: Blockade of CCL1 inhibits T regulatory cell suppressive function enhancing tumor immunity without affecting T effector responses. *J Immunol* 2010, 184:6833–6842
61. Karin N: Chemokines and cancer: new immune checkpoints for cancer therapy. *Curr Opin Immunol* 2018, 51:140–145
62. Ge X, Zhao Y, Chen C, Wang J, Sun L: Cancer immunotherapies targeting tumor-associated regulatory T cells. *Onco Targets Ther* 2019, 12:11033–11044